GRAIN REFINEMENT TECHNIQUES TO REDUCE BIODEGRADATION RATE OF MAGNESIUM ALLOY AS A POTENTIAL BIODEGRADABLE IMPLANT MATERIAL: A REVIEW

Nanang Qosim[1], Silmina Adzhani[2]

[1]Department of Mechanical Engineering, Faculty of Engineering, Universitas Indonesia
Kampus Baru UI, Depok16424, Indonesia
[2]Department of Mechanical Engineering, Graduate School of Engineering,
Tokyo Metropolitan University
1 Chome-1 Minamiosawa, Hachioji, Tokyo 192-0364, Japan
nanang.qosim@ui.ac.id

ABSTRACT

As a lightweight metal with mechanical properties similar to natural bone, magnesium-based material has been gaining wide popularity. However, the applications are seriously limited due to the excessively rapid degradation rate in the physiological environment, causing the magnesium to degrade faster than the complete rehabilitation of the bone itself. Grain refinement approach is currently the selected approach to obtain a lower degradation rate without adding other element that might be harmful to human body. This paper studies the possibility of reducing biodegradation rate of a biodegradable through reviewing various studies on grain refinement through hot deformation and rapid solidification.

Keywords: magnesium, biodegradation rate, grain refinement, hot deformation, rapid solidification.

INTRODUCTION

Today, more than 200 years after the first production of metallic magnesium by Sir Humphry Davy in 1808, as a lightweight metal with mechanical properties similar to natural bone, magnesium-based materials as potential candidates for degradable temporary implants have been gaining wide popularity (Witte, 2015, Staiger et al., 2006). The dominant reason is because of their mechanical properties which are close to that of natural bone compared to other metals, their good biocompatibility, nontoxicity and biodegradability (Staiger et al., 2006, Witte,

2015, Henderson et al., 2014, Chaya et al., 2015, Witte et al., 2008). Many new magnesium alloys and composites have been produced and evaluated for biomaterial applications (Mueller et al., 2010, Hermawan, Sunil et al., 2014a, Sunil et al., 2014b, Kirkland and Birbilis, 2014, Keim et al., 2011). However, the applications are seriously limited due to the excessively rapid degradation rate in the physiological environment (Staiger et al., 2006, Mueller et al., 2010, Keim et al., 2011, Witte et al., 2006, Wang et al., 2008). Previous studies have been shown that the grain size of Mg alloys

can be refined by hot deformation methods such as extrusion, rolling, double extrusion (DE), backward extrusion (BE), cyclic extrusion and compression (CEC), high pressure torsion (HPT) process, equal channel angular pressing (ECAP), etc. due to dynamic recrystallization (Jinfeng et al., 2014, Zakiyuddin et al., 2014, Gao et al., 2011, Wang et al., 2010). Furthermore, rapid solidification is another effective way to refine the microstructures of Mg alloys (Wang et al., 2010, Willbold et al., 2013, Liao et al., 2012).

Since the late 1930s, a number of approaches have been developed to obtain grain refinement in magnesium alloys that contain aluminum. These are briefly summarized as hot plastic deformation and rapid solidification. Hot plastic deformation is a useful method to refine grains and obtain a homogeneous microstructure. A fine microstructure can often be achieved by common deformation, such as single extrusion (SE) and rolling (Jinfeng et al., 2014, Zakiyuddin et al., 2014). Moreover, when Gao et al. (2011) studied the corrosion behavior of the Mg-Zn-Ca alloy in SBF using an HPT process, they found that the second phase has been refined to nano-sized particles and distributed homogeneously in the interior of α-Mg grains. As a result, the alloy shows a uniform corrosion mode, indicating that severe plastic deformation is also useful for improving the corrosion mode of Mg alloys.

Rapid solidification has been shown to refine the microstructure of Mg alloys due to the increased solidification rate (Wang et al., 2010, Willbold et al., 2013). The corrosion resistance is also enhanced by rapid solidification because of grain refinement and fine dispersion of the quasi-crystals and intermetallic compounds in the α-Mg matrix. Liao, et. al. (Liao et al., 2012) studied the corrosion resistance of the Mg-Al-Mn-Ca alloy (AMX602) by rapid solidification and found that the corrosion rate of the alloy produced by the spinning water atomization process is 2.5–10 times less than that of the hot-extruded and as-cast alloy. Izumi et. al. (Izumi et al., 2009) proposed that increasing the cooling rate can reduce filiform corrosion of the Mg-Zn-Y alloy due to grain refinement and formation of a supersaturated single α-Mg solid solution. In addition, rapid solidification can improve microstructural and electrochemical homogeneities of Mg-Zn-Y alloys as well as enhance the passivity of substrate materials, leading to a reduction of the occurrence of local breakdown of films.

METHODS

a) The experiment studying electrochemical performance of AZ31 magnesium alloy under different processing

As This experiment was conducted by Jinfeng, D. et. al. (Jinfeng et al., 2014). AZ31 magnesium alloys were used in the experiment. The extruded, rolled, cast-rolled, as-cast AZ31 magnesium alloys were prepared as the working electrode,

respectively. Electrolyte used in the experiment was 3.5% (mass fraction) NaCl. Electrochemical performance tests were carried through the electro-chemical workstation. The samples (30 mm×10 mm×0.6 mm) were successively polished, carefully degreased with acetone and rinsed with distilled water and alcohol, followed by ultrasonic cleaning for 5 min. Then the samples were packed with the acrylic acid, leaving the work area of 10 mm×10 mm as the work electrode, after-ward dried by warm air for later use. The microstructures and morphologies of the corroded surfaces were analyzed using optical microscope and SEM coupled with EDS system. The sample after free corrosion test was cleaned by distilled water and ultrasonic washing before SEM test. Self-discharge rate can be expressed as:

$$J = \frac{(m_0 - m_1) \times 2 \times 96500}{24St} \tag{1}$$

Where J is free corrosion rate, mA/cm2; m0 is initial mass and m1 is accurate mass of samples after self-corrosion test, mg; t is for time, s; S is area, cm2. Electrochemical impedance spectroscopy (EIS) was measured in the frequency range of 10-1~105 Hz.

b) The experiment studying of homogeneous corrosion of high-pressure torsion treated Mg–Zn–Ca alloy in simulated body fluid

Gao et. al. (Gao et al., 2011) experimented using the alloy with a chemical composition of Mg-2 wt.%Zn-0.24 wt.% Ca that was prepared from pure Mg (99.99%),

zinc (99.98%) and Ca (99.98%), using an electric resistance heating furnace. The melt was cast into a steel mold. The samples used for HPT treatment were cut from the as-cast magnesium alloys with a diameter of 10 mm and a thickness of 0.6 mm. Each disk was compressed and deformed in a mold with a diameter of 10 mm between the two anvils under an applied pressure of 5 GPa at room temperature to a total of five complete revolutions. The samples for transmission electron microscope (TEM) investigation were cut from the disks at a distance of 2.5 mm from the sample center using diamond cutter. The ingot was extruded at 593 K with an extrusion ratio of 17.4:1 into a magnesium bar with a diameter of 12 mm to prepare extruded samples. The potentiodynamic polarization experiments were conducted on a chemical workstation (RST5200). Both the potentiodynamic polarization experiments and the immersion tests were carried out in Kokubo's SBF (Kokubo and Takadama, 2006) in a water bath at 37 °C. The scan rate of the potentiodynamic polarization experiments was 0.5 mV/s. Before the corrosion tests, all samples were firstly ground with SiC papers progressively to 800 grits followed by ultrasonically cleaning in ethanol for 15 min and then embedded into the epoxy resin with only one side of 1 cm2 exposed. For the HPT treated samples, one side was exposed and the exposed area was 0.785 cm2. In the immersion tests, each prepared sample was

placed in a sterilized bottle containing 20 ml SBF solution.

c) The experiment studying the improvement of corrosion resistance of high-strength Mg-Al-Mn-Ca magnesium alloy made by rapid solidification

The experiment was conducted by Liao J. et. al. (Liao et al., 2012) using AMX602. ASTM-specified AZ31B alloy was also used as a reference. Each AMX602 samples with three different fabricated methods which are SWAP, gravity cast and hot-extrusion were investigated. Firstly, the as-cast AM602 alloy was atomized by the spinning water atomization to produce an extremely high solidification rate about 106 K/s, which resulted in powders with fine microstructure and supersaturation of alloying elements. Then the atomized powders were collected and consolidated to billets by cold compaction at room temperature using a pressure of 400 MPa, and subsequently hot-extruded to rods and plates (0.5 mm/s at temperature of 573-623 K).

d) The experiment studying of rapidly solidified magnesium alloy RS66 as a temporary biodegradable metal

Elmar W. et al. (Willbold et al., 2013) experimented on RS66, a magnesium-based alloy with a nominal composition of Mg–6.0% Zn–1.0% Y–0.6% Ce–0.6% Zr and extraordinary physicochemical properties of high tensile strength combined with a high ductility and a homogeneous grain size of ~1 μm which was obtained by rapid

solidification processing and reciprocal extrusion. The study analyzed the biodegradation behavior and the biocompatibility of this alloy.

e) The experiment studying of micro-structure and corrosion properties of as sub-rapid solidification Mg-Zn-Y-Nd alloy in dynamic simulated body fluid for vascular stent application

Jun W. et al. (Wang et al., 2010) experimented on a Mg–Zn–Y–Nd alloy. Samples was prepared by using high purity Mg, high purity Zn, Mg–25Y (wt%) (in purity 99.99 wt%) and Mg–25Nd (wt%) (in purity 99.97 wt%) master alloys by induction of mild steel crucible at approximately 740℃ under CO_2/SF_6 (volume fraction rate, 3000:1) atmosphere in an electronic resistance furnace. The sub- rapidly solidified bars were prepared by copper mold splat cooling method at 700℃ under Ar atmosphere. The diameter of the bars was 2 mm. The cooling rate range of sub-rapid solidification is 102–103K/S, and the cooling rate of Φ2mm bars was about 200 K/s, which come within the cooling rate range of sub-rapid solidification.

DISCUSSIONS

a) The experiment studying electrochemical performance of AZ31 magnesium alloy under different processing

Fig.1 shows the optical microstructures of the AZ31 magnesium alloy under different processing conditions. The as-cast grains are

apparently coarser and larger than the others. The extruded sample exhibits relatively fine grains. The grains of the rolled magnesium alloy are roughly equiaxed and disperse uniformly. The rolled and cast-rolled alloys have irregular grain boundaries and the grains do not disperse uniformly compared to those of extruded magnesium alloys. There are no obvious twins in the four states of magnesium alloys.
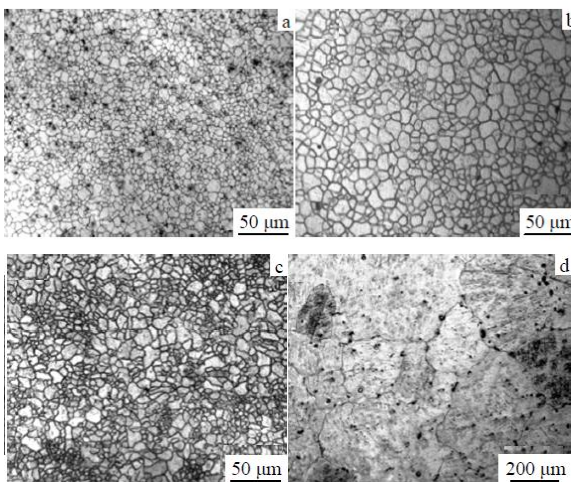
Fig.1 Metallographs of AZ31 magnesium alloy under different processing conditions: (a) extruded, (b) rolled, (c) cast-rolled, and (d) as-cast (Jinfeng et al., 2014)

The corrosion rates of AZ31 magnesium alloy under different processing conditions immersed in 3.5% NaCl solution for 70 h are shown in Table 2. The extruded sample exhibits the lowest corrosion rate among the four, followed by the rolled and cast-rolled magnesium alloys. The corrosion of the as-cast AZ31 magnesium alloy is heavy. This result is consistent with the polarization curves.

Table.1 Free corrosion of AZ31 magnesium alloy in 3.5% NaCl solution (Jinfeng et al., 2014)

Material	Free corrosion rate/Ma.cm^{-2}
Extruded	0.054
Rolled	0.095
Cast-rolled	0.099
As-cast	0.143

b) The experiment studying of homogeneous corrosion of high-pressure torsion treated Mg–Zn–Ca alloy in simulated body fluid

Fig. 2(a) displays the microstructure of the as-cast alloy. The average grain size was appropriately 97 μm and the second phase continuously distributed along the grain boundaries. The microstructures of the samples after conventional extrusion and HPT treatment are shown in Fig. 2(b) and (c), respectively. After the conventional extrusion, the grain size was about 5.4 μm (Fig. 2(b)) and most of the second phase still continuously located at the grain boundaries and numerous micro-sized second-phase particles were also observed in grain interiors. However, after the HPT treatment a large number of nano-sized second phase particles precipitated in the grain interiors and the average grain size of α-Mg was about 1.2 μm (Fig. 2(c)). And no second phase was found at grain boundaries after HPT treatment due to the redistribution and reduction of the second phase.
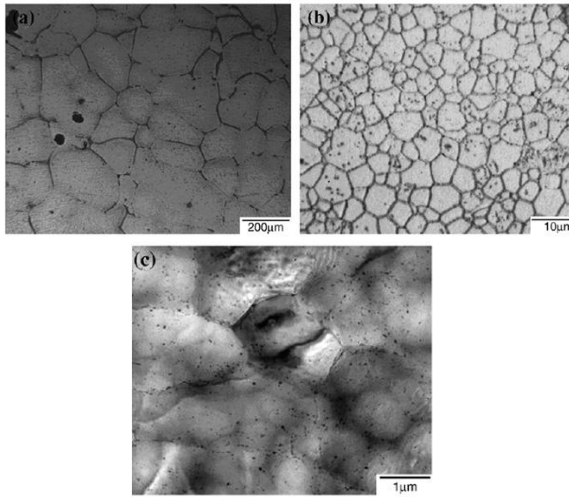
Fig. 2. Optical images for: (a) as-cast, (b) conventional extrusion alloy and (c) TEM for HPT-treated alloy (Gao et al., 2011)
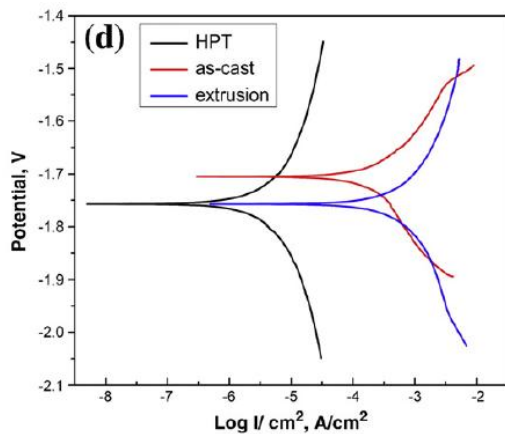
Fig 3. potentiodynamic curves of as-cast, conventional extrusion and HPT-treated alloys (Gao et al., 2011)

The corrosion behavior of the as-cast, conventional extrusion, and HPT-treated alloy were also studied by potentiodynamic polarization. The potentiodynamic curves are shown in Fig. 3. Compared with the as-cast Mg–Zn–Ca alloy, the corrosion current density of HPT-treated alloy decreased from 5.3×10^{-4} A/cm2 to 3.3×10^{-6} A/cm2 but its corrosion potential shifted to a more negative value. However, the current density of the sample treated by conventional extrusion

was increased, and at the same time its corrosion potential became more negative compared with the as-cast alloy. According to Faraday's Law (Wen et al., 2009), it can be found that the HPT-treated samples possessed the lowest biodegradation rate, followed by as-cast and conventional extrusion alloys and this result was consistent with the immersion test.

c) The experiment studying the improvement of corrosion resistance of high-strength Mg-Al-Mn-Ca magnesium alloy made by rapid solidification

Based on the experiment results, it is found that the SWAPed alloy has not only superior mechanical properties but also distinguished corrosion resistance. The SWAPed alloy has extremely fine α-Mg grains (0.8–1 μm) and fine dispersed Al2Ca particles (smaller than 100 nm) and the ratio of Al2Ca phase to Mg matrix is much lower in the SWAPed alloy as compared to the as-cast and extruded. Because of the different microstructures of the three AMX602 alloys, their corrosion rates are very different (Figs. 5 and 6).

The SWAPed AMX602 alloy shows the extremely low corrosion rate about 10 and 2.5 times higher than that of the as-cast and extruded alloys respectively in 0.1 M NaCl solution, or 4 and 3.4 times higher respectively in cyclic neutral-salt spray test.
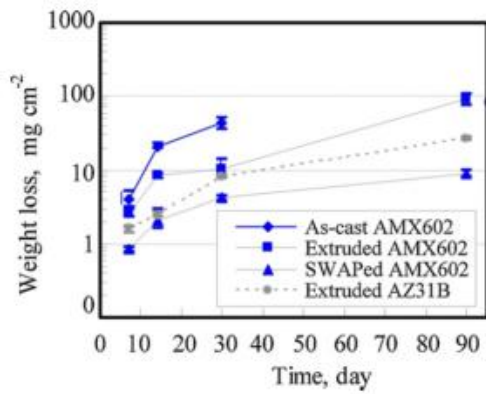
Fig 4. Immersion test results in 0.1 M NaCl solution. (Liao et al., 2012)
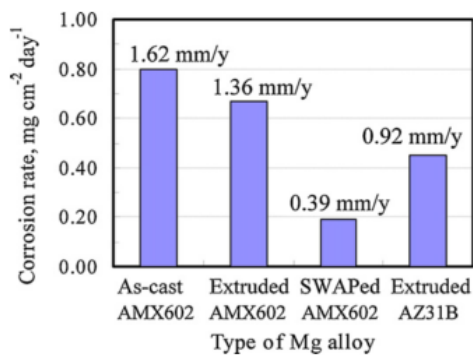
Fig 5. Cyclic neutral-salt spray test results (Liao et al., 2012)
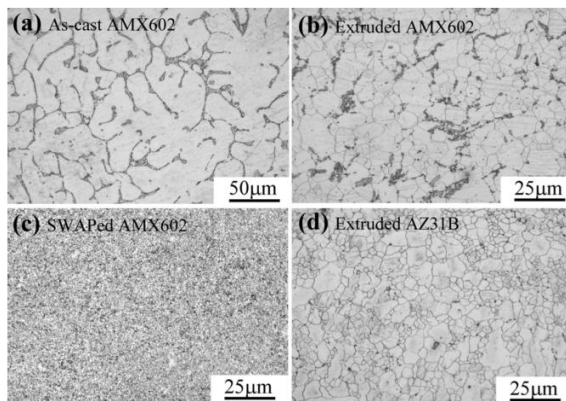
Fig 6. Microstructure of mg alloys: (a) as-cast AMX602, (b) extruded AMX602, (c) SWAPed AMX602 and (d) AZ31B. (Liao et al., 2012)

The results show, the Al2Ca phase is dispersed and somewhat refined by extrusion in the extruded AMX602 alloy, and the Al2Ca phase is extremely refined and dispersed in the SWAPed alloy. The refinement and

dispersion of intermetallic phase can suppress the cathodic reaction and thereby improve the corrosion resistance of magnesium alloys (Figs. 7 and 8).
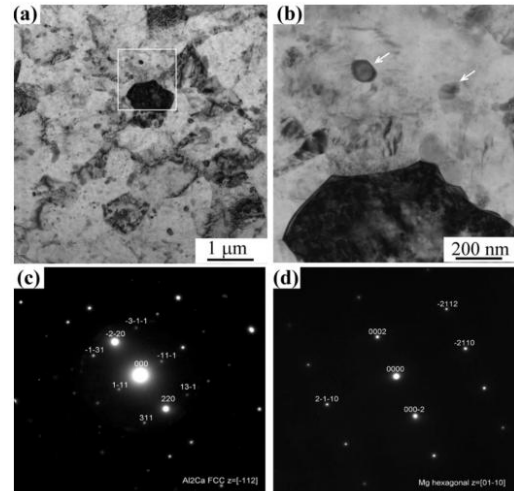
Fig 7. TEM micrograph and electron diffraction pattern of Mg matrix and dispersed intermetallic particle in SWAPed AMX602 alloy (Liao et al., 2012)

d) The experiment studying of rapidly solidified magnesium alloy RS66 as a temporary biodegradable metal

This study demonstrated that the slowly degrading magnesium alloy RS66, produced by rapid solidification, showed a sufficient biocompatibility in physiological environments both in vitro and in vivo. In vitro, pure extract medium or 1:2 dilutions both reduced the viability and proliferation and were cytotoxic to primary human osteoblasts. This observation is most probably related to the very high ion concentrations and the subsequent high osmotic strength of the extract medium. Also, a pH shift to non-physiological high values may play a role (Yang et al., 2010). In future work, specific investigation of coatings for

soft tissue applications and fabricate implants for fracture healing are needed.

e) The experiment studying of micro-structure and corrosion properties of as sub-rapid solidification Mg-Zn-Y-Nd alloy in dynamic simulated body fluid for vascular stent application

It is shown in the optical microstructures that the grain size of as-cast alloys is not uniform and the size of larger grains is even beyond 150 μm (Fig 9). Comparison of the average grain size of samples with the same compositions under different process conditions, both Mg–Y–Gd–Nd and Mg–Zn–Y–Nd alloys, after sub-rapid solidification, their grains refine obviously, that is, the increasing cooling rate results solute closure, grain size decrease notably and more phases appear, in the meanwhile, elements distribute more uniform.

Table 2. Relationship of corrosion potential and corrosion current (Wang et al., 2010)

Samples		E_{corr}/V	$I_{corr}(A/cm^2)$
Mg-Y-Gd-Nd alloy	As cast	-1.95	1.86×10^{-4}
	As sub-rapid solidification	-1.83	1.45×10^{-4}
Mg-Zn-Y-Nd alloy	As cast	-1.76	5.30×10^{-4}
	As sub-rapid solidification	-1.57	2.62×10^{-4}

Based on the results, the corrosion properties of Mg–Zn–Y–Nd alloys, as sub-rapid solidification or as cast, are better than the Mg–Y–Gd–Nd alloys. The main reasons are that: Firstly, as sub-rapid solidification Mg–Zn–Y–Nd alloys exist I-phase which is favorable to improve the corrosion properties, because it has low interfacial energy making it have stable interface; secondly, I-phase own excellent corrosion properties itself; Thirdly, it has been widely accepted that Zn can reduce the effects of Fe, Ni on corrosion properties and then improve the anticorrosion properties of Mg.

CONCLUSION

Fast corrosion rates and localized corrosion modes remain major obstacles for magnesium-based materials use in clinical application, a problem that cannot be solved using only surface-altering technologies. Therefore, more attention should be paid to the improvement of the intrinsic corrosion behavior of the material. Several effective processes can be used to modify the corrosion behavior during the preparation of Mg alloys, such as rapid solidification and hot deformation as grain refinement processes. There is great potential for the use of these grain refinement methods for further application in medical field.

REFERENCES

Chaya, A., Yoshizawa, S., Verdelis, K., Myers, N., Costello, B. J., Chou, D.-T., Pal, S., Maiti, S., Kumta, P. N. & Sfeir, C. 2015. In vivo study of magnesium plate and screw degradation and bone fracture healing. *Acta biomaterialia,* 18**,** 262-269.

Gao, J., Guan, S., Ren, Z., Sun, Y., Zhu, S. & Wang, B. 2011. Homogeneous corrosion of high pressure torsion treated Mg–Zn–Ca alloy in simulated body fluid. *Materials Letters,* 65**,** 691-693.

Henderson, S. E., Verdelis, K., Maiti, S., Pal, S., Chung, W. L., Chou, D.-T., Kumta, P. N. & Almarza, A. J. 2014. Magnesium alloys as a biomaterial for degradable craniofacial screws. *Acta biomaterialia,* 10**,** 2323-2332.

Hermawan, H. Biodegradable Metals: From concept to applications. 2012. New York: Springer.

Izumi, S., Yamasaki, M. & Kawamura, Y. 2009. Relation between corrosion behavior and microstructure of Mg–Zn–Y alloys prepared by rapid solidification at various cooling rates. *Corrosion Science,* 51**,** 395-402.

Jinfeng, D., Guangsheng, H., Yanchun, Z. & Bei, W. 2014. Electrochemical performance of AZ31 magnesium alloy under different processing conditions. *Rare Metal Materials and Engineering,* 43**,** 316-321.

Keim, S., Brunner, J. G., Fabry, B. & Virtanen, S. 2011. Control of magnesium corrosion and biocompatibility with biomimetic coatings. *Journal of Biomedical Materials Research Part B: Applied Biomaterials,* 96**,** 84-90.

Kirkland, N. T. & Birbilis, N. 2014. *Magnesium Biomaterials: Design, Testing, and Best Practice*, Springer.

Kokubo, T. & Takadama, H. 2006. How useful is SBF in predicting in vivo bone bioactivity? *Biomaterials,* 27**,** 2907-2915.

Liao, J., Hotta, M. & Mori, Y. 2012. Improved corrosion resistance of a high-strength Mg–Al–Mn–Ca magnesium alloy made by rapid solidification powder metallurgy. *Materials Science and Engineering: A,* 544**,** 10-20.

Mueller, W.-D., Nascimento, M. L. & De Mele, M. F. L. 2010. Critical discussion of the results from different corrosion studies of Mg and Mg alloys for biomaterial applications. *Acta biomaterialia,* 6**,** 1749-1755.

Staiger, M. P., Pietak, A. M., Huadmai, J. & Dias, G. 2006. Magnesium And Its Alloys as orthopedic biomaterials: a review. *Biomaterials,* 27**,** 1728-1734.

Sunil, B. R., Ganapathy, C., Kumar, T. S. & Chakkingal, U. 2014a. Processing and mechanical behavior of lamellar structured degradable magnesium–hydroxyapatite implants. *Journal of the mechanical behavior of biomedical materials,* 40**,** 178-189.

Sunil, B. R., Kumar, T. S., Chakkingal, U., Nandakumar, V. & Doble, M. 2014b. Nano-hydroxyapatite reinforced AZ31 magnesium alloy by friction stir processing: a solid state processing for biodegradable metal matrix composites. *Journal of Materials Science: Materials in Medicine,* 25**,** 975-988.

Wang, J., Wang, L., Guan, S., Zhu, S., Ren, C. & Hou, S. 2010. Microstructure and corrosion properties of as sub-rapid solidification Mg–Zn–Y–Nd alloy in dynamic simulated body fluid for vascular stent application. *Journal of Materials Science: Materials in Medicine,* 21**,** 2001-2008.

Wang, Y., Wei, M., Gao, J., Hu, J. & Zhang, Y. 2008. Corrosion process of pure magnesium in simulated body fluid. *Materials letters,* 62**,** 2181-2184.

Wen, Z., Wu, C., Dai, C. & Yang, F. 2009. Corrosion behaviors of Mg and its alloys with different Al contents in a modified simulated body fluid. *Journal of Alloys and Compounds,* 488**,** 392-399.

Willbold, E., Kalla, K., Bartsch, I., Bobe, K., Brauneis, M., Remennik, S., Shechtman, D., Nellesen, J., Tillmann, W. & Vogt, C. 2013. Biocompatibility of rapidly solidified magnesium alloy RS66 as a temporary biodegradable metal. *Acta biomaterialia,* 9**,** 8509-8517.

Witte, F. 2015. Reprint of: The history of biodegradable magnesium implants: A review. *Acta biomaterialia,* 23**,** S28-S40.

Witte, F., Fischer, J., Nellesen, J., Crostack, H.-A., Kaese, V., Pisch, A., Beckmann, F. & Windhagen, H. 2006. In vitro and in vivo corrosion measurements of magnesium alloys. *Biomaterials,* 27**,** 1013-1018.

Witte, F., Hort, N., Vogt, C., Cohen, S., Kainer, K. U., Willumeit, R. & Feyerabend, F. 2008. Degradable biomaterials based on magnesium corrosion. *Current opinion in solid state and materials science,* 12**,** 63-72.

Yang, C., Yuan, G., Zhang, J., Tang, Z., Zhang, X. & Dai, K. 2010. Effects of magnesium alloys extracts on adult human bone marrow-derived stromal cell viability and osteogenic differentiation. *Biomedical Materials,* 5**,** 045005.

Zakiyuddin, A., Yun, K. & Lee, K. 2014. Corrosion behavior of as-cast and hot rolled pure magnesium in simulated physiological media. *Metals and Materials International,* 20**,** 1163-1168.